Effect of PVP content and polymer concentration on polyetherimide (PEI) and polyacrylonitrile (PAN) based ultrafiltration membrane fabrication and characterization

Sevgi Güneş-Durak, Türkan Ormancı-Acar and Neşe Tüfekci

ABSTRACT

In this study, four different membranes were fabricated by using polyetherimide and polyacrylonitrile polymers, N-methyl-2-pyrrolidone and polyvinylpyrrolidone (PVP) via phase inversion method to improve the membrane performance in fruit juice wastewater (FJWW) treatment. The addition of PVP to the casting solution increased membrane hydrophilicity, water content, contact angle, porosity, Fourier transform infrared spectroscopy peaks, membrane thickness, average roughness and viscosity of cast solutions compared to the bare membrane. It can be said that the addition of a lower polymer concentration and PVP intensively increases the pure water flux of the membrane. However, as the flux increased, a small decrease in FJWW rejection was observed.

Key words | fruit juice wastewater, membrane characterization, phase inversion, PVP, ultrafiltration

Sevgi Güneş-Durak (corresponding author)
Faculty of Architecture and Engineering,
Department of Environmental Engineering,
Nevsehir Hacı Bektas Veli University,
50300 Nevsehir,
Turkey
E-mail: *sgdurak@nevsehir.edu.tr*

Türkan Ormancı-Acar
Neşe Tüfekci
Faculty of Engineering, Department of Environmental Engineering,
Istanbul University,
Istanbul,
Turkey

INTRODUCTION

The choice of suitable polymer in membrane fabrication plays a key role for the ultrafiltration (UF) membrane. Polyetherimide (PEI) and polyacrylonitrile (PAN) polymers are known as a good candidate for forming a good UF membrane structure.

PEI has structural and mechanical properties such as excellent film formation, moderate chemical and good thermal resistance (Trewjumrone & Chinpa 2010).

PAN polymer has a satisfactory chemical stability in filtration implementations. Commercial membranes, which are often marketed commercially, need to be kept wet at all times. If the membranes dry, membrane pores collapse, and the membrane material becomes brittle which causes sudden breaking during the filtration (Scharnagl & Buschatz 2001). PAN membranes with high pure water permeability are generally prepared in the form of flat sheets by selecting a suitable component of the casting solution and the preparation conditions (Wu *et al.* 2000). However, in the industrial wastewater treatment, pervaporation process, and production of the composite membranes substrate, PAN membranes are being used aplenty because of their tolerance to organic solvents (Qin *et al.* 2004).

Polyvinylpyrrolidone (PVP) is a water-soluble polymer. It is often used as a pore-forming agent in the preparation of asymmetric membranes by phase inversion method. It is used to modulate the structures of the membranes by affecting the polymer membranes (Wan *et al.* 2006). PVP provides morphology control in terms of the thermodynamics and the kinetics for polymer membranes. In thermodynamics, it makes the structure of polymer inconsistent and inclined to the phase separation. Kinetically, phase differentiation/discretization of the high viscosity of the polymer solution will provide a lagged and decelerated demixing process by PVP addition (Zhang *et al.* 2011). Furthermore, PVP addition increases membrane selectivity by reducing relative transport rate or failures at the membrane surface (Rao *et al.* 2008). The molecular structure of PEI, PAN and PVP polymers is given in Figure 1 (Sigma Aldrich).

The variability of casting solution viscosity, membrane pore size, and membrane porosity are defined as a function of the casting solution constituent (Dal-Cin *et al.* 1994). There are a lot of studies about blended PEI-PVP (Salleh & İsmail 2011; Bakeri *et al.* 2015; Hebbar *et al.* 2015) and blended PAN-PVP (Nouzaki *et al.* 2002; Jung *et al.* 2004; Yang & Lin 2002).

The phase inversion method has been widely used (Machado *et al.* 1999; Kim *et al.* 2002; Zheng *et al.* 2006). In this method, the polymer dissolves in a solvent at various times and temperatures to form a viscous solution. This

doi: 10.2166/wst.2018.142

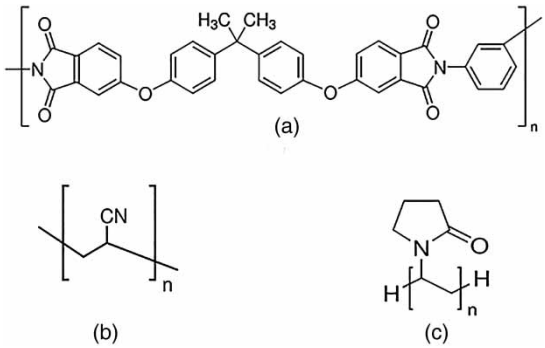

Figure 1 | Molecular structure of (a) PEI, (b) PVP and (c) PAN.

method is based on the exchange of solvent and nonsolvent on diffusion and causes the cast solution to make a phase transition leading to the formation of the membrane (Young & Chen 1995). Membrane structure and morphology are related to kinetic parameters such as solvent–nonsolvent exchange (Tsai *et al.* 2002; Li *et al.* 2008). Furthermore, thermodynamic parameters such as polymer/solvent interactions, solvent/nonsolvent interactions, evaporation time and coagulation bath temperature affect the membrane formation mechanism significantly (Amirilargani *et al.* 2010). To increase membrane performance and enhance the phase inversion method, additives such as PVP can be added to the base polymer and solvent mixture (Al Malek *et al.* 2012).

Fruit juice wastewater is formed during the stages of fruit juice production: pressing, container washing, filtration and grinding of the juice. The characteristics of the fruit juice wastewater in the literature are shown in Table 1 (El-Kamah *et al.* 2010).

Carbohydrates the primary components of juice content: food sugar, food acid and low molecular weight sweetener components. Sugar accounts for up to 20% of the water-soluble components of fruit juices. Organic acid and inorganic salts are present in lower amounts (0.1 to 2%). Many volatile components such as alcohol, aldehyde, ketone and ester are contained in very small quantities in fruit juice. The high amount of sugar present in the solution in the membrane filtration causes a flux decrease due to the high osmotic pressure of the sugar solution. Due to the high viscosity of the feed solution, there is also a reduction in the mass transfer coefficient of the membrane (Rana *et al.* 2014).

In this study, the asymmetric membrane fabrication was performed using PEI and PAN polymers, PVP as pore forming agents and N-methyl-2-pyrrolidone (NMP) as a solvent. For membrane fabrication, wet phase inversion method was used. After preparation, the performances of the membranes were tested by treating fruit juice wastewater

Table 1 | Main characteristics of fruit juice wastewater

Parameters	Unit	Min	Max	Average
pH-value	–	5.4	8	–
COD	mg/L	2,280	10,913	5,157 ± 2,897
BOD_5	mg/L	1,650	6,900	3,134 ± 1,546
TSS (105 °C)	mg/L	118	1,534.0	323 ± 349
VSS (550 °C)	mg/L	14	580	183 ± 152.4
TDS (105 °C)	mg/L	2,304	17,918	5,483 ± 3,941
TKN	mg/L	38.0	252	58.2 ± 59
Total phosphorous	mg/L	4.6	20.8	10.2 ± 5.3
Oil and grease	mg/L	18.0	717.8	74 ± 180
Sulfate	mg/L	72	214	144.3 ± 59
Hydrogen sulfide	mg/L	0.0	20.0	10.7 ± 9
Iron	mg/L	0.1	4.4	1.03 ± 1.5
Chloride	mg/L	80	1,000	260 ± 271

COD: chemical oxygen demand; BOD_5: biochemical oxygen demand; TSS: total suspended solids; VSS: volatile suspended solids; TKN: total Kjeldahl nitrogen.

(FJWW). According to the results, the effect of polymer and PVP concentrations on water flux and rejection were investigated and evaluated. Fourier transform infrared (FTIR) spectroscopy, scanning electron microscopy (SEM), atomic force microscopy (AFM), water contact angle, viscosity, porosity and water content methods have been used for characterization of membrane structure.

EXPERIMENTAL

Materials

PEI (CAS Number 61128-46-9) is a polymer which has 30,000 g/mol average molecular, and PAN (CAS Number 25014-41-9) is a polymer which has the average molecular weight of 150,000 g/mol. They were purchased from Sigma Aldrich. NMP (8060722500) was purchased from Merck. In the preparing of PEI and PAN membranes, in order to increase pore size and improve permeability of membranes PVP10 was used as an additive. PVP10 (CAS Number 9003-39-8) was purchased from Sigma Aldrich.

Preparation of membranes

For preparing PEI_0 membranes, a casting solution of 20 wt.% of PEI polymer and 80 wt.% of NMP was used. PVP-added membrane casting solution was prepared including 12 wt.%

of PEI, 8 wt.% of PVP and 80 wt.% NMP. For the casting solution of PAN membranes, the solution of PAN_0 membrane comprised 15 wt.% of PAN and 85 wt.% of NMP, and the solution of the PAN_8 membrane comprised 10 wt.% of PAN, 8 wt.% of PVP and 82 wt.% of NMP (Table 2).

For the preparation of the PEI_0 casting solution, PEI polymer was added to NMP, and then the mixture was stirred for 24 h at 40 °C with 110 rpm to obtain a homogeneous solution. During PEI_8 membrane preparation, firstly PVP was added to NMP; after the dissolution of PVP, the solution was added with PEI and the new solution was stirred for 24 h at 40 °C in 110 rpm centrifuge velocity. Similarly, PAN_0 and PAN_8 membrane mixtures were stirred for 24 h at room temperature at 90 rpm. After the solution reached a homogeneous phase, before membrane solution casting to a glass plate, we ensured that air bubbles were removed.

Membrane casting solutions were cast on the glass plate and using knife gab of 200 μm, were cut properly. After 10 seconds, the glass plate was immediately immersed in distilled water for coagulation at room temperature. After this process, prepared membranes were kept in water and a cold room until their use in the membrane bioreactor (MBR) system.

Membrane characterization

Viscosity

To measure the viscosity of PEI_0, PEI_8, PAN_0 and PAN_8, a Brookfield DV-E viscometer was used. The measurement was carried out at 100 s^{-1} shear rate for 2 min at 20 °C using cone/plate geometry.

Porosity measurements

For PEI_0, PEI_8, PAN_0, and PAN_8, porosity measurements were carried out by the dry–wet method and calculated using the expression in Equation (1).

$$\text{Porosity} = \frac{w_w - w_d}{v.d_{water}} \times 100\% \quad (1)$$

w_w: weight of membrane (after dipping into distilled water) (g),
w_d: weight of dry membrane (g),
v: volume of the membrane in the wet state (cm^3),
d_{water}: density of distilled water at room temperature (g/cm^3).

Table 2 | Composition (wt.%) of membrane casting solutions

	Solution composition, wt.%			
Component	**PEI_0**	**PEI_8**	**PAN_0**	**PAN_8**
PEI	20	12	0	0
PAN	0	0	15	10
NMP	80	80	85	82
PVP	0	8	0	8

Water content

Water content measurements for all membrane types were done by the dry–wet method. In this method, unlike the porosity calculation method, the membrane, which was left in distilled water for 24 hours, was dried with drying paper and then the wet weight was measured. For dry weight, the measurement was carried out after the membrane was kept in a 45 °C incubator for 48 hours. It was calculated by the expression given in Equation (2):

$$\text{water content } (\%) = \frac{W_w - W_d}{W_w} \times 100 \quad (2)$$

w_w: weight of membrane (after dipping into distilled water for 24 h at room temperature and drying by filter paper) (g),
w_d: weight of membrane (after being in the incubator at 45 °C for 48 h) (g).

Contact angle measurements

To characterize the membrane surface polarity, an Attension T200 Theta was used. At room temperature, using a droplet of 5 μL on the membrane surface, the measurement was carried out. After three different measurements on the membrane surface, the mean of three values was used.

Fourier transform infrared spectroscopy

FTIR spectra for each membrane were recorded with a Perkin Elmer Spectrum 100 TIR spectrophotometer. The spectral range of this spectrophotometer is 40–4,000 cm^{-1} and resolution is 4 cm^{-1} scan. The probes used were 1,2-dichloroethane, 1,1,2,2-tetrabromoethane, and 1,2-diphenylethane. The procedures for the preparation of polymer films,

determination of their thickness, the introduction of probes into them, and the estimation of the concentration of probes are similar to those described in Kamalova *et al.* (2008).

Scanning electron microscopy

The membranes were examined by SEM using an FEI Quanta 450 FEG-EDS. The emission cathode was operated at 0.2–30 kV. Before SEM analyses, membranes were cut by cold nitrogen.

Atomic force microscopy

AFM of PEI, PVP-added PEI, PAN and PVP-added PAN membranes was carried out using a Digital Instruments atomic force microscope.

Pure water flux

Water flux measurements were performed using a membrane bioreactor. The effective area of all membranes was 49 cm^2 and the operation was carried out at 20 °C and 600 mbar pressure. The water flux was calculated by Equation (3).

$$J = \frac{Q}{A\Delta t} \tag{3}$$

J: water flux (L/(m^2 h)),
Q: quantity of permeate collected after the membrane reached the steady state (L),
Δt: sampling time (h),
A: membrane area (m^2).

Flux and percentage rejection

A series rejection model was used for rejection calculations (Chang & Lee 1998). Firstly, in order to determine the rejection of membranes due to their structure, distilled water was passed through the clean membranes. The flux–time graphs were drawn to determine the rejection value (R_m) of the membranes, and the total rejection (R_t) value was obtained by filtering FJWW through the membranes. In Figure 2 a schematic diagram of the flow is given.

RESULTS

Viscosity measurements

The viscosity of casting solutions of PEI_0, PEI_8, PAN_0 and PAN_8 was measured to control membrane morphology. If the phase inversion process is used for the membrane, polymer solution viscosity becomes an important factor for the membrane morphology. Solutions with higher viscosity are more compatible with a slower diffusion between the phase conversion components, because there is a delayed exchange between solvent and nonsolvent.

Casting solution viscosity of membranes was decreased with the PVP addition. Although the amount of PVP added to the polymers is the same, the viscosity of the membrane casting solutions is reduced. This may be due to a reduction in the amount of polymer in weight (wt.%) in the casting solution. But many researchers have reported that adding PVP into the casting solution increased the viscosity (Torrestiana-Sánchez *et al.* 1999; Yuan & Dan-Li 2008; Alpatova *et al.* 2013). Han & Nam (2002) have found that when the amount of polymer is kept constant and the

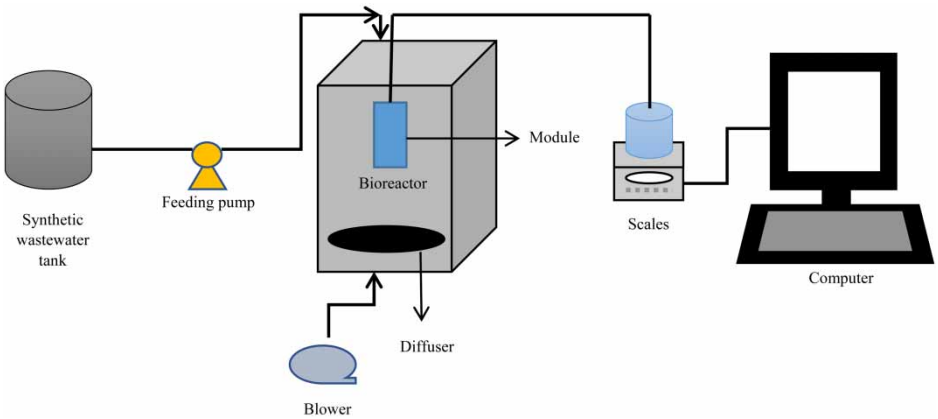

Figure 2 | The schematic diagram of the flow of MBR system.

content of NMP in the solution decreases, the viscosity of the casting solution increases with increasing PVP amount. In this study, the decrease in the viscosity of the casting solution was considered to be due to the decrease in the amount of polymer, since the amount of polymer was reduced and PVP was added to the casting solution. When PVP is added and PVP-free membranes are compared, the viscosity of the membrane decreases as more polymer is reduced, while the viscosity of the membrane decreases as less polymer is reduced in proportion to the amount of polymer (Table 3).

In addition, increased water content and increased hydrophobicity of PVP-added membranes can be considered as factors that lead to decreased viscosity.

It is known that as the viscosity of membrane casting solution increases, the thickness of the initial membrane increases. However, in this study, as the viscosity decreases due to PVP addition, the porosity-causing membrane thickness increases (Table 4) (Fathizadeh *et al.* 2012). In addition, the weight reduction of the main polymer amount, but the increase in the total amount of polymer by weight with the addition of PVP, may have resulted in an increase in membrane thickness (Mustaffar *et al.* 2004). The viscosity value of PEI_0 was first measured as 2.82 Pa.s, but after the addition of PVP, the viscosity of PEI_8 decreased to 1.19 Pa.s. The thickness of the PEI_0 membrane was 1.7 mm while it increased to 2.1 mm by the addition of PVP. Similarly, the viscosity value of PAN_0 was first measured as 2.80 Pa.s, but after the addition of PVP, the viscosity of PAN_8 decreased to 2.04 Pa.s. The thickness of the PAN_0 membrane was 1 mm while it increased to 1.7 mm by the addition of PVP.

Table 3 | Polymer amounts and viscosity change for all fabrication membranes

Polymers	Polymer amounts (wt.%)	Viscosity change (%)
$PEI_0 \rightarrow PEI_8$	$20 \rightarrow 12$	−57.8
$PAN_0 \rightarrow PAN_8$	$15 \rightarrow 10$	−39.3

Table 4 | Properties of membrane casting solutions and membranes

Membrane	Water content (%)	Contact N-methyl-2-pyrrolidonengle (°)	Pore size (μm)[a]	Porosity (%)	Thickness (mm)
PEI_0	72	19	0.8	74	1.7
PEI_8	84	78	0.8	77	2.1
PAN_0	86	16	0.3	23	1.0
PAN_8	90	50	0.2	51	1.7

[a]SEM analyses.

Water content and porosity

When all membranes were analyzed, membrane water content and membrane porosity increased with decreasing weight of the main polymer (Table 4). In addition, there was a significant decrease in PAN_0 porosity with increasing main polymer amount. When PVP was added and polymer concentration was decreased, values of contact angle were increased. However, there was no significant change in pore size for all membranes with the addition of PVP. While the water content of the PEI_0 membrane was 72%, the water content of the PEI_8 membrane increased to 84% as a result of the PVP addition. The contact angle increased from 19% to 78% and the porosity increased from 74% to 77%.

Contact angle measurement

According to Table 4, the contact angle of membranes increased by using PVP as an additive. In addition, in the absence of PVP, pure membranes presented less hydrophilicity (Wan *et al.* 2006). The contact angle for PEI_0 membrane was 19° and for PEI_8 was 78°. The contact angle for PAN_0 was 16°, and for PAN_8 was 50°. Table 4 shows that the addition of PVP to PEI and PAN polymers increases contact angle values and decreases membrane hydrophilicity. When polymer PVP is added in membrane fabrication the contact angle increases significantly. Since PVP polymer is more hydrophobic compared to PEI and PAN polymers, PVP presence in the membrane structure causes membrane hydrophilicity to be reduced. In addition, the contact angle value is reduced due to the reduction of the main polymer concentration (Table 2) (Ochoa *et al.* 2003).

However, the molecular weight of PVP used in this study is low. For this reason, it can be said that a part of PVP is retained in the membrane pores and affects the structure of the membrane (Saljoughi & Mohammadi 2009).

Fourier transform infrared spectroscopy

Figure 3 depicts the FTIR absorption spectra of PEI_0, PEI_8, PAN_0, and PAN_8. FTIR spectra of pure PEI fibers have many peaks which are related to the existence of C = O, C–N, C–N–C and C–O bonds. The typical imide bands can be detected at 1,717 cm^{-1} (symmetric and asymmetric imide C = O stretching, respectively). C–N–C absorption of

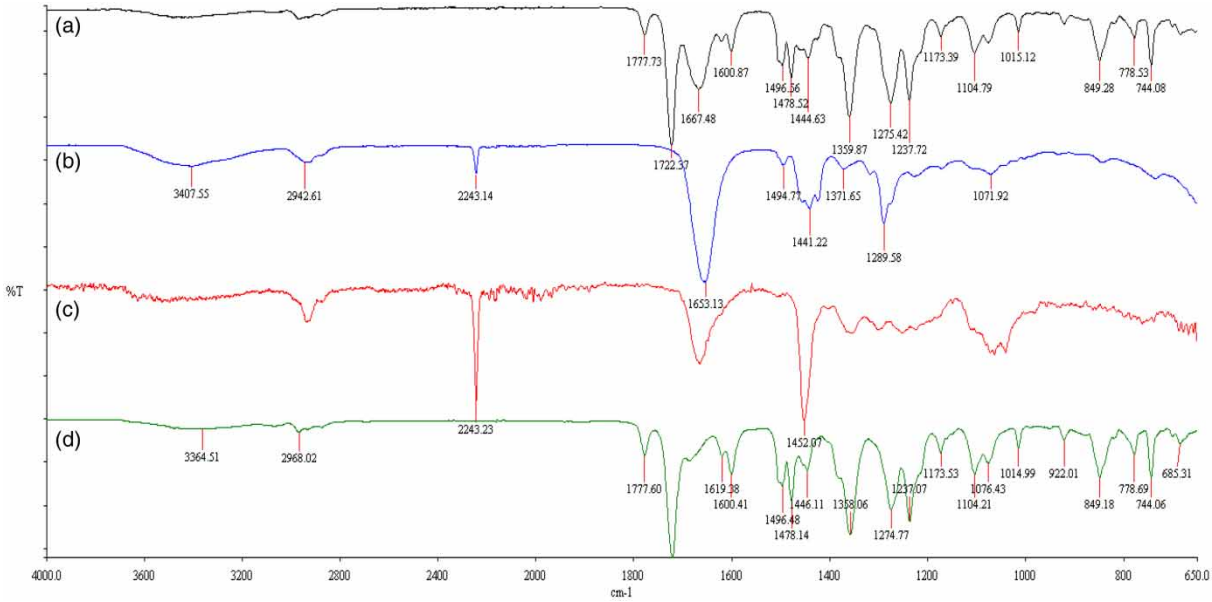

Figure 3 | FTIR spectra of (a) PEI_8, (b) PAN_8, (c) PAN_0 and (d) PEI_0.

the imide ring was observed at 1,357 cm^{-1}. The C–O stretching appears at 1,236 cm^{-1} and the C–N stretching appears at 743 cm^{-1} (Trewjumrone & Chinpa 2010). After adding PVP to PEI membrane, many peaks occurred at 1,444, 1,478, 1,496, 1,600, 1,667, 1,722 and 1,777 cm^{-1}. The C–O stretching at 1,236 cm^{-1} has disappeared. The peak at 1,444 cm^{-1} may be related to C–H and O–H deformation vibrations (Lamsal *et al.* 2012). The absorption bands at 1,478 cm^{-1} correspond to the C–N vibration of the quaternary ammonium (Sánchez *et al.* 2013). The reason for the peak formation at 1,496–1,600 cm^{-1} is the presence of –C = C bonds, and the peak at 1,667 cm^{-1} is due to –C = N bond stretching (Farsani *et al.* 2009). At 1,722 cm^{-1} and 1,777 cm^{-1}, C = O and –C = N stretching was observed (Mungali *et al.* 2015). And at these peaks, the FTIR spectrum showed the appearance of characteristic imide bands.

PAN_0 showed two peaks at 1,452 and 2,243 cm^{-1}: the characteristic nitrile (C ≡ N) peak at 2,243 cm^{-1} and deformation at 1,452 cm^{-1}, respectively (Majeed *et al.* 2012). After adding PVP to PAN membrane, many peaks occurred at 1,071, 1,289, 1,371, 1,441, 1,494, 1,668, 2,942 and 3,407 cm^{-1}. But the peak which is at 1,452 cm^{-1} disappeared. The absorption peak around 3,407 cm^{-1} is related to O–H, NH and COO–H bonds. Another peak was observed around 2,942 cm^{-1} (nitrile bonds, C ≡ N). C = N and C = C bonds are situated at 1,668 cm^{-1}. The strongest peak at 1,668 cm^{-1} arising from the carbonyl group (C = O) stretching vibration in PVP can be regarded as the typical peaks of PVP (Wan *et al.* 2006; Farsani *et al.* 2009). Absorption in the range of 1,441 and 1,494 cm^{-1} is related to tensile vibration and peaks in the range of 1,289–1,371 cm^{-1} are related to vibration in a different situation. Another peak was observed at 1,071 cm^{-1} which is related to presence of C = O or C–O bonds and is caused by the co-monomers' presence (Farsani *et al.* 2009).

SEM analyses

Membrane thickness and cross-section structure were measured by SEM. To dissolve the precise section of the membrane, a prepared membrane was cut in the shape of a rectangle and immediately immersed in liquid nitrogen and used for sectioning. The surfaces and cross-sectional shapes of PEI_0, PEI_8, PAN_0, and PAN_8 membranes are shown in Figure 4(a)–4(d) respectively.

Depending on the different chemical properties, it can be observed that the size of the microporous structure decreases when blending PEI and PAN with PVP (Figure 4(b) and 4(d)). According to these images, finger-like structures can be said to be present due to the addition of PVP in PEI membranes (PEI_8) (Yoo *et al.* 2004). All membranes have characteristic asymmetric structures consisting of layers with cellular morphology added to the polymer matrix, as well as strata engaging with asymmetric finger-like pores (Balta *et al.* 2012). From the SEM analysis, it is seen that the pore size of PEI_0 and PEI_8 membranes is larger than the pore size of PAN_0 and PAN_8 membranes (Table 4).

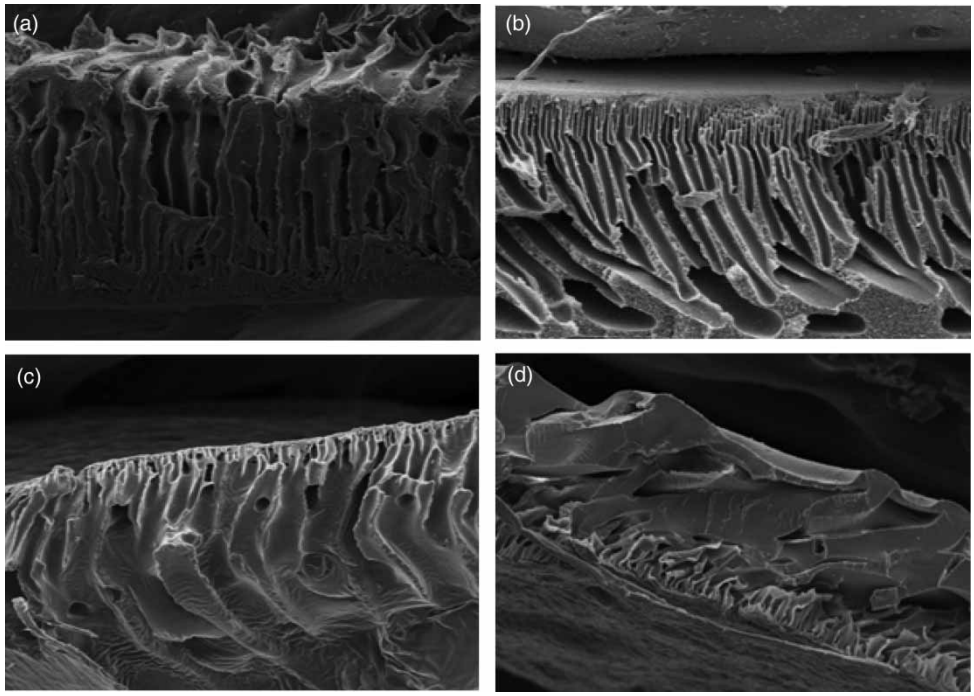

Figure 4 | SEM images of cross-sectional structures of (a) PEI_0, (b) PEI_8, (c) PAN_0 and (d) PAN_8 (10.00 kV, 600×, 100 μm).

Atomic force microscopy

The surface roughness of the membranes was determined using AFM. Surface roughness parameters, expressed as mean roughness (RMS), the mean square of the Z data (R_a) and mean difference of the five highest peaks and the lowest five peaks (R_z), were calculated (Table 5).

According to the measurement results, the roughness of PVP-added membranes was markedly higher than PEI_0 and PAN_0. The three-dimensional topography is given in Figure 5(a)–5(d). The surface of PEI_8 and PAN_8 appears intensely and finely dispersed under gravity. This means that PEI_8 and PAN_8 have a rougher surface. PEI_0 and PAN_0 have a smoother surface. While all membranes, especially PEI_0, were examined, it was observed that the nodule structure of all membranes exhibited a heterogeneous nodule agglomerate distribution (Kanagaraj *et al.* 2015). In addition, as shown in Figure 5(a) and 5(c), the size of the nodules of PEI_0 and PAN_0 is slightly smaller than that of PEI_8 and PAN_8.

Because of membrane structural nodules formed from polymer aggregates, surface roughness often affects membrane performance (Shehzad *et al.* 2015). Studies indicate that the roughness of the membrane affects the increase in flux and permeability as the surface roughness increases (Johnson & Hilal 2015).

Table 5 | Roughness measurements of all membranes

Membrane	RMS (nm)	R_a (nm)	R_z (nm)
PEI_0	14.77	11.03	64.68
PEI_8	42.5	29.94	121.39
PAN_0	14.94	11.91	65.61
PAN_8	36.14	27.77	97.45

Pure water permeability

The pure water fluxes (PWFs) of PEI_0, PEI_8, PAN_0, and PAN_8 were measured at 0.6 bar transmembrane pressure. Figure 6 shows the PWF of the PEI_0, PEI_8, PAN_0 and PAN_8.

Initially, PEI_0 presented the lowest value of PWF (26 L/(m^2 h)) and PAN_8 presented the highest value of PWF (545 L/(m^2 h)). When the PVP was added to the casting solution, the PWF values of the membranes increased (for PEI_0 from 26 to 160 L/(m^2 h) and for PAN_0 from 281 to 545 L/(m^2 h)). This can be explained by the increased number of pores and size of pores due to the presence of PVP, because PVP acted as a pore-forming agent during the phase inversion. PVP is a hydrophilic polymer but when the characterization of PVP-added membranes is examined, contact angle values of membranes show that they become hydrophobic.

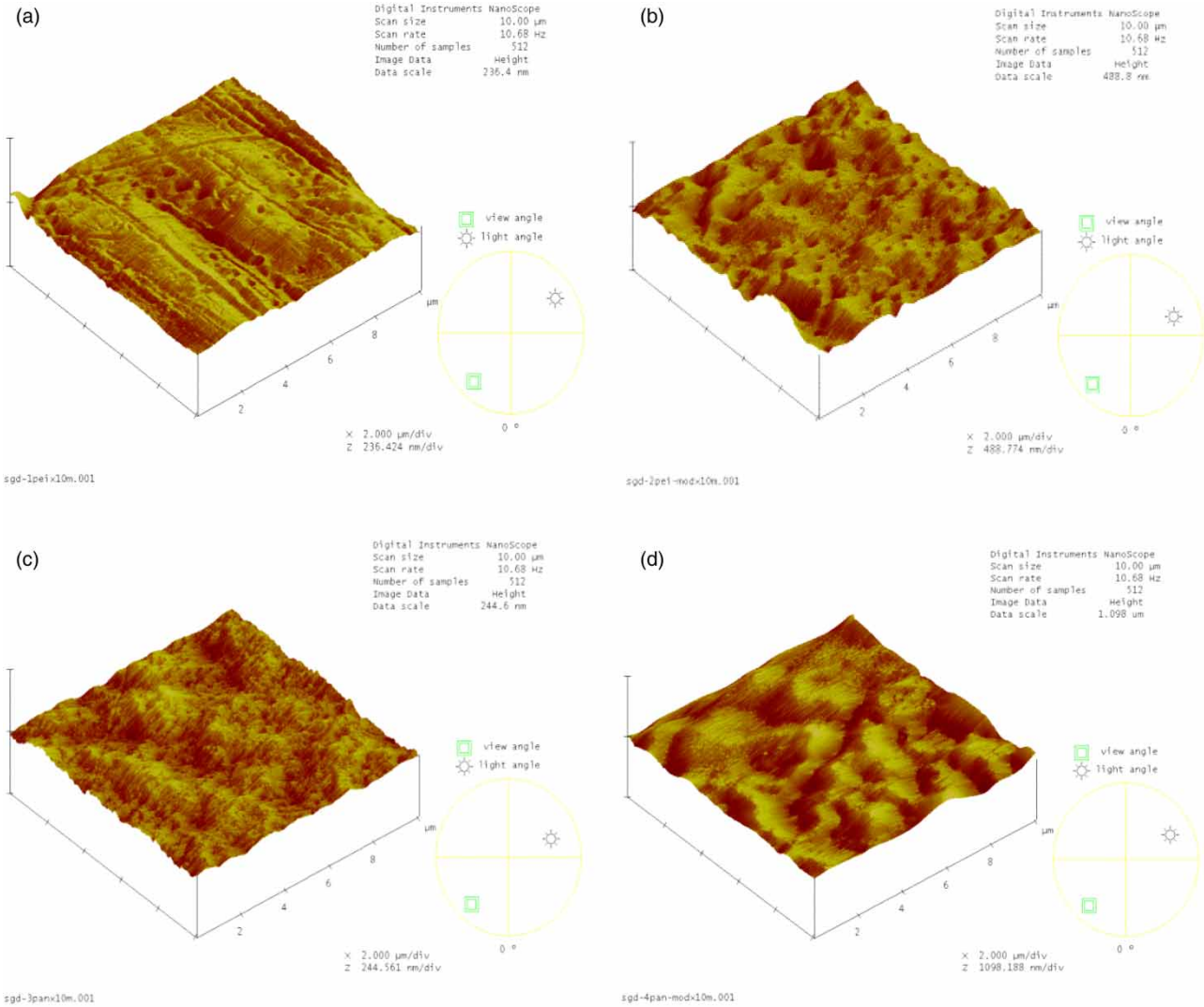

Figure 5 | Three-dimensional AFM images of (a) PEI_0, (b) PEI_8, (c) PAN_0 and (d) PAN_8.

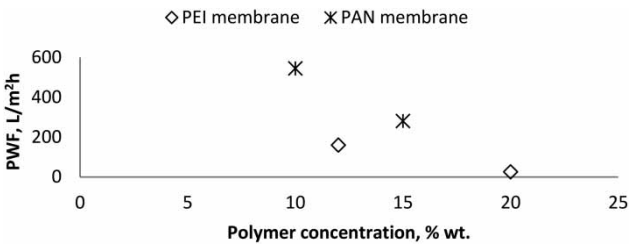

Figure 6 | Effect of polymer concentration on PWF.

The highest membrane permeability is obtained for PAN_8. When PEI_0 and PEI_8 are compared, it is possible to see that PEI_0 provides less permeability. It may be the result of decreasing of PEI polymer concentration. The same situation is encountered in the membranes PAN_0 and PAN_8 (The PAN polymer in the membrane casting solution for PAN_8 membrane fabrication was reduced by 33%.) (Kanagaraj *et al.* 2015).

Figure 6 shows the effect of different formulations on PWP with different polymer concentrations. According to Figure 6, when the polymer concentration was increased from 10% to 15% by weight for the PAN membrane and from 12% to 20% by weight for the PEI membrane, the average PWF was reduced.

Flux and percentage rejection

In this study, FJWW was used to determine flux and rejection values of membranes. The sludge age of the juice wastewater is 30 days and the COD value is 1,000 mg/L. Figure 7 shows the total rejection, membrane rejection and

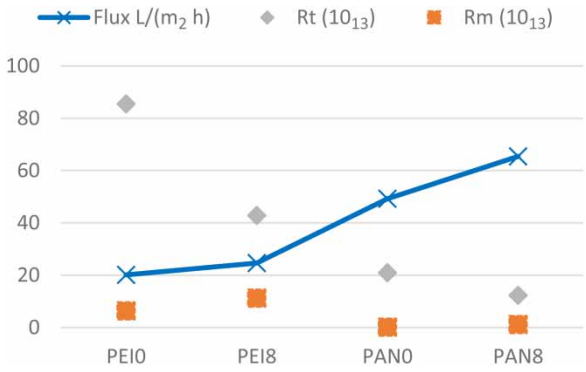

Figure 7 | Effect of polymer concentration on percentage rejection.

FJWW treatment flux values. FJWW treatment flux was similar to PWP behavior. As the wt.% of the PEI and PAN polymers in the casting solution decreased, the FJWW treatment flux increased. According to Figure 7, a mean flux of 65 L/(m^2 h) was obtained for the PAN polymer containing 10 wt.% polymer (PAN_8). In the case of a membrane containing 15 wt.% polymer (PAN_0), the average flux value was determined to be 49 L/(m^2 h). For PEI, when the polymer concentration was 12% by weight, the mean flux value was 25 L/(m^2 h), whereas for polymer concentration of 20% it was 20 L/(m^2 h). However, the PWF values were increased by PVP addition to the polymers.

The effect of different polymer concentration on total rejection and membrane rejection is shown in Figure 7. The total rejection percentage of the PEI membrane was 8.55×10^{14}, while it decreased to 4.28×10^{14} after PVP was added. The total rejection percentage of the PAN membrane was 2.09×10^{14} but decreased to 1.23×10^{14} after PVP was added.

When all of the PEI_0, PEI_8, PAN_0 and PAN_8 membranes were examined, there was a decrease in the percent membrane rejection by decreasing the main polymer concentration (PEI and PAN). It is also possible to say that PVP addition increases the percentage of membrane rejection, because the concentration of the main polymer, with respect to PEI_0 and PAN_0, was reduced in PEI_8 and PAN_8 membranes. With the addition of PVP, the rejection of the PEI membrane increased from 6.32×10^{13} to 11.2×10^{13} and the rejection of the PAN membrane increased from 0.1×10^{13} to 1.1×10^{13}. Thus, PVP addition has an adverse effect on total rejection and membrane rejection.

CONCLUSIONS

In this study, membranes were prepared with PVP as an additive, NMP as a solvent and water as a coagulation bath. The permeability of the membranes was checked by PVP addition. When the results are examined, it has been found that PVP addition and reduction of polymer concentration increase membrane permeability and membrane water content. The chemical structure, morphology, and surface roughness were investigated using FTIR spectroscopy, SEM, and AFM. Adsorption peaks and membrane surface roughness increase with the addition of PVP and lowering of the main polymer concentration. SEM analyses showed that the pore size of PEI_0 and PEI_8 was larger than the pore size of PAN_0 and PAN_8. Thus, it can be said that PVP does not affect the membrane pore size. This result can be explained by the PEI polymer structure (the molecular weight of the PEI polymer is lower than the molecular weight of the PAN polymer). PVP-added membranes were observed to be rougher by the AFM. In particular, there was a significant increase in PAN_0 porosity (121%). A decrease in solution viscosity was observed with the addition of PVP. This can be explained by the fact that the main amount of polymer is not kept constant but reduced. In addition, pure membranes provide a hydrophilic surface when PVP is not present. However, the hydrophilicity of the membrane surface was reduced by PVP addition and the membrane showed a hydrophobic tendency. The PWF of the membranes increased when the PVP addition was sufficient and the polymer concentration was reduced.

To determine the resistance of the membranes to wastewater, FJWW with a 30-day sludge age and a concentration of 1,000 mg/L COD was used. When the performances obtained from the membranes in the wastewater treatment system are examined, it is determined that, when PVP is added and the main polymer concentration decreases, the FJWW treatment flux increases and the total rejection decreases. However, the membrane rejection increases with the PVP addition.

ACKNOWLEDGEMENTS

This project has been funded with support from Istanbul University Scientific Research Projects (15210/2011).

REFERENCES

Al Malek, S. A., Abu Seman, M. N., Johnson, D. & Hilal, N. 2012 Formation and characterization of polyethersulfone membranes using different concentrations of polyvinylpyrrolidone. *Desalination* **288**, 31–39.

Alpatova, A., Kim, E.-S., Sun, X., Hwang, G., Liu, Y. & El-Din, M. G. 2013 Preparation of porous polymeric nanocomposite membranes with enhanced anti-fouling properties: effect of casting composition. *Journal of Membrane Science* **444**, 449–460.

Amirilargani, M., Saljoughi, E., Mohammadi, T. & Moghbeli, M. R. 2010 Effects of coagulation bath temperature and polyvinylpyrrolidone content on flat sheet asymmetric polyethersulfone membranes. *Polymer Engineering and Science* **50**, 885–893.

Bakeri, Gh., İsmail, A. F., Rezaei DashtArzhandi, M. & Matsuura, T. 2015 Porous PES and PEI hollow fiber membranes in a gas–liquid contacting process – a comparative study. *Journal of Membrane Science* **475**, 57–64.

Balta, S., Sotto, A., Luis, P., Benea, L., van der Bruggena, B. & Kim, J. 2012 A new outlook on membrane enhancement with nanoparticles: the alternative of ZnO. *Journal of Membrane Science* **389**, 155–161.

Chang, I. S. & Lee, C. H. 1998 Membrane filtration characteristics in membrane coupled activated sludge system – the effect of physiological states of activated sludge on membrane fouling. *Desalination* **120**, 221–233.

Dal-Cin, M., Tam, C. M., Guiver, M. & Tweddle, T. A. 1994 Polysulfone membranes. V. Poly(phenyl sulfone) (Radel r)-poly(vinylpyrrolidone) membranes. *Journal of Applied Polymer Science* **54**, 783–792.

El-Kamah, H., Tawfik, A., Mahmoud, M. & Abdel-Halim, H. 2010 Treatment of high strength wastewater from fruit juice industry using integrated anaerobic/aerobic system. *Desalination* **253** (1–3), 158–163.

Farsani, R. E., Raissi, S., Shokuhfar, A. & Sedghi, A. 2009 FT-IR study of stabilized PAN fibers. *World Academy of Science, Engineering and Technology* **50**, 42–48.

Fathizadeh, M., Aroujaliana, A. & Raisi, A. 2012 Effect of lag time in interfacial polymerization on polyamide composite membrane with different hydrophilic sub layers. *Desalination* **284**, 32–41.

Han, M.-J. & Nam, S.-T. 2002 Thermodynamic and rheological variation in polysulfone solution by PVP and its effect in the preparation of phase inversion membrane. *Journal of Membrane Science* **202** (1–2), 55–61.

Hebbar, R. S., İsloor, A. M., İsmail, A. F., Shilton, S. J., Obaid, A. & Fun, H.-K. 2015 Probing the morphology and anti-organic fouling behaviour of a polyetherimide membrane modified with hydrophilic organic acids as additives. *New Journal of Chemistry* **39**, 6141–6150.

Johnson, D. & Hilal, N. 2015 Characterisation and quantification of membrane surface properties using atomic force microscopy: a comprehensive review. *Desalination* **356**, 149–164.

Jung, B., Yoon, J. K., Kim, B. & Rhee, H. W. 2004 Effect of molecular weight of polymeric additives on formation, permeation properties and hypochlorite treatment of asymmetric polyacrylonitrile membranes. *Journal of Membrane Science* **243**, 45–57.

Kamalova, D. I., Kolyadko, I. M., Remizov, A. B., Galimullin, D. Z. & Salakhov, M. Kh. 2008 The local dynamics of polyetherimides: conformational probes, IR Fourier transform spectra, and quantum-chemical calculations. *Russian Journal of Physical Chemistry A. Focus on Chemistry* **82** (12), 2085–2091.

Kanagaraj, P., Nagendran, A., Rana, D., Matsuura, T., Neelakandan, S., Karthikkumar, T. & Muthumeenal, A. 2015 Influence of N-phthaloyl chitosan on poly (ether imide) ultrafiltration membranes and its application in biomolecules and toxic heavy metal ion separation and their antifouling properties. *Applied Surface Science* **329**, 165–173.

Kim, I. C., Yoon, H. G. & Lee, K. H. 2002 Formation of integrally skinned asymmetric polyetherimide nanofiltration membranes by phase inversion process. *Journal of Applied Polymer Science* **84**, 1300–1307.

Lamsal, R., Harroun, S. G., Brosseau, C. L. & Gagnon, G. A. 2012 Use of surface enhanced Raman spectroscopy for studying fouling on nanofiltration membrane. *Separation and Purification Technology* **96**, 7–11.

Li, Z., Tang, H., Liu, X., Xia, Y. & Jiang, J. 2008 Preparation and characterization of microporous poly(vinyl butyral) membranes by supercritical CO_2-induced phase separation. *Journal of Membrane Science* **312**, 115–124.

Machado, P. S. T., Habert, A. C. & Borges, C. P. 1999 Membrane formation mechanism based on precipitation kinetics and membrane morphology: flat and hollow fiber polysulfone membranes. *Journal of Membrane Science* **155**, 171–183.

Majeed, S., Fierro, D., Buhr, K., Wind, J., Du, B., Boschetti-de-Fierro, A. & Abetz, V. 2012 Multi-walled carbon nanotubes (MWCNTs) mixed polyacrylonitrile (PAN) ultrafiltration membranes. *Journal of Membrane Science* **403–404**, 101–109.

Mungali, M., Pandey, V., Arif, M. & Singh, K. P. 2015 Construction of anti omp immobilized nanoporous membrane based electrochemical biosensor for the detection of *E. coli*. *Global Journal of Multidisciplinary Studies* **4** (4), 96–102.

Mustaffar, M. I., İsmail, A. F. & Illias, R. M. 2004 Study on the effect of polymer concentration on hollow fiber ultrafiltration membrane performance and morphology. In: *Regional Symposium on Membrane Science and Technology, Malaysia, 2004*.

Nouzaki, K., Nagata, M., Arai, J., Idemoto, Y., Koura, N., Yanagishita, H., Negishi, H., Kitamoto, D., Ikegami, T. & Haraya, K. 2002 Preparation of polyacrylonitrile ultrafiltration membranes for wastewater treatment. *Desalination* **144**, 53–59.

Ochoa, N. A., Masuelli, M. & Marchese, J. 2003 Effect of hydrophilicity on fouling of an emulsified oil wastewater with PVDF/PMMA membranes. *Journal of Membrane Science* **226** (1–2), 203–211.

Qin, J.-J., Cao, Y.-M., Li, Y.-Q., Li, Y., Oo, M.-H. & Lee, H. 2004 Hollow fiber ultrafiltration membranes made from blends of PAN and PVP. *Separation and Purification Technology* **36** (2), 149–155.

Rana, D., Matsuura, T. & Sourirajan, S. 2014 Physicochemical and engineering properties of food in membrane separation processes. In: *Engineering Properties of Foods*, 4th edn (M. A. Rao, S. S. H. Rizvi, A. K. Datta & J. Ahmed, eds). Taylor & Francis/CRC Press, Boca Raton, FL, USA, pp. 437–525.

Rao, P. S., Wey, M. Y., Tseng, H. H., Kumar, I. A. & Weng, T. H. 2008 A comparison of carbon nanotube molecular sieve membrane with polymer carbon molecular sieve membranes for the gas separation application. *Microporous Mesoporous Materials* **113**, 499–510.

Saljoughi, E. & Mohammadi, T. 2009 Cellulose acetate (CA)/ polyvinylpyrrolidone (PVP) blend asymmetric membranes: preparation, morphology and performance. *Desalination* **249** (2), 850–854.

Salleh, W. N. W. & İsmail, A. F. 2011 Carbon hollow fiber membranes derived from PEI/PVP for gas separation. *Separation and Purification Technology* **80** (3), 541–548.

Sánchez, J., Toledo, L., Rivas, B. L., Rivera, N. & Muñoz, E. 2013 Water-soluble cationic cellulose coupled to a ultrafiltration membrane for the removal of arsenic and chromium. *Journal of the Chilean Chemical Society* **58** (4), 1986–1990.

Scharnagl, N. & Buschatz, H. 2001 Polyacrylonitrile (PAN) membranes for ultra- and microfiltration. *Desalination* **139**, 191–198.

Shehzad, M. A., Qaiser, A. A., Javaid, A. & Saeed, F. 2015 In situ solution-phase polymerization and chemical vapor deposition of polyaniline on microporous cellulose ester membranes: AFM and electrical conductivity studies. *Synthetic Metals* **200**, 164–171.

Torrestiana-Sánchez, B., Ortiz-Basurto, R. İ. & Brito-De La Fuente, E. 1999 Effect of nonsolvents on properties of spinning solutions and polyethersulfone hollow fiber ultrafiltration membranes. *Journal of Membrane Science* **152**, 19–28.

Trewjumrone, W. & Chinpa, W. 2010 Surface modification of poly (ether imide) support membrane for preparation of anti-fouling ultrafiltration membrane. *The Journal of KMUTNB* **20** (1), 28–36.

Tsai, H. A., Hong, M. J., Huang, G. S., Wang, Y. C., Li, C. L., Lee, K. R. & Lai, J. Y. 2002 Effect of DGDE additive on the morphology and pervaporation performances of asymmetric PSf hollow fiber membranes. *Journal of Membrane Science* **208**, 233–245.

Wan, L.-S., Xu, Z.-K. & Wang, Z.-G. 2006 Leaching of PVP from polyacrylonitrile/PVP blending membranes: a comparative study of asymmetric and dense membranes. *Journal of Polymer Science Part B: Polymer Physics* **44** (10), 1490–1498.

Wu, K.-F., Qiu, P., Wang, Z.-J. & Wang, J.-R. 2000 Large pore size polyacrylonitrile membrane for ultrafiltration. *Journal of Environmental Sciences* **12** (4), 478–481.

Yang, M.-C. & Lin, W.-C. 2002 Surface modification and blood compatibility of polyacrylonitrile membrane with immobilized chitosan–heparin conjugate. *Journal of Polymer Research* **9** (3), 201–206.

Yoo, S. H., Kim, J. H., Jho, J. Y., Won, J. & Kang, Y. S. 2004 Influence of the addition of PVP on the morphology of asymmetric polyimide phase inversion membranes: effect of PVP molecular weight. *Journal of Membrane Science* **236** (1–2), 203–207.

Young, T. H. & Chen, L. W. 1995 Pore formation mechanism of membranes from phase inversion process. *Desalination* **103**, 233–247.

Yuan, Z. & Dan-Li, X. 2008 Porous PVDF/TPU blends asymmetric hollow fiber membranes prepared with the use of hydrophilic additive PVP (K30). *Desalination* **223**, 438–447.

Zhang, P. Y., Wang, Y. L., Xu, Z. L. & Yang, H. 2011 Preparation of poly (vinyl butyral) hollow fiber ultrafiltration membrane via wet-spinning method using PVP as additive. *Desalination* **278**, 186–193.

Zheng, Q. Z., Wang, P., Yang, Y. N. & Cui, D. J. 2006 The relationship between porosity and kinetics parameter of membrane formation in PSF ultrafiltration membrane. *Journal of Membrane Science* **286**, 7–11.

First received 2 November 2017; accepted in revised form 14 March 2018. Available online 27 March 2018